

EFFICIENT EVALUATION OF ELLIPSOIDAL HARMONICS FOR POTENTIAL MODELING

THOMAS S. KLOTZ, JAYDEEP P. BARDHAN, AND MATTHEW G. KNEPLEY

ABSTRACT. Ellipsoidal harmonics are a useful generalization of spherical harmonics but present additional numerical challenges. One such challenge is in computing ellipsoidal normalization constants which require approximating a singular integral. In this paper, we present results for approximating normalization constants using a well-known decomposition and applying tanh-sinh quadrature to the resulting integrals. Tanh-sinh has been shown to be an effective quadrature scheme for a certain subset of singular integrands. To support our numerical results, we prove that the decomposed integrands lie in the space of functions where tanh-sinh is optimal and compare our results to a variety of similar change-of-variable quadratures.

1. INTRODUCTION

Ellipsoidal harmonics are eigenfunctions of the Laplacian in ellipsoidal coordinates [9, 13, 10], and are thus related to the spherical harmonics which are the eigenfunctions for spherical coordinates. In fact, in ellipsoidal coordinates, the Laplace equation is separable into three identical equations, the only coordinate system for which this is true [16]. Expansions in ellipsoidal harmonics are suited for problems in potential theory with distributions or boundaries that are well-modeled by ellipsoids. Unfortunately, ellipsoidal harmonics can be difficult to use, compared to their spherical counterparts. Some of these difficulties include a lack of closed-form solutions for high-order harmonics, normalization constants which are defined by a singular integral, multi-valued coordinate transforms, and other implementation-specific details. For example, all computations in ellipsoidal coordinates depend on the problem-specific choice of semi-axis lengths and must be performed again for each choice of semi-axes.

Despite computational challenges, ellipsoidal harmonics provide many computational benefits. First, if the region of interest is better described by an ellipsoid, say a non-spherical comet [18], then the expansion will converge in areas much closer to the region of interest than will spherical harmonics. Thus in our example, we can calculate the gravitational field much closer to our comet. Second, even in volumes for which both expansion converge, the rate of convergence, as a function of order of the expansion, can be higher for ellipsoidal harmonics.

The numerics of expansion in ellipsoidal harmonics have been examined in prior work [7]. However, calculation of the normalization constants for the expansion was both an accuracy and efficiency bottleneck. In this paper, we present a method for calculating the singular integrals which defines the normalization constants with tanh-sinh quadrature. This method is particularly suitable for high-order ellipsoidal harmonics since accuracy is only limited by the precision of interior harmonic evaluations. In Section 2, we review the ellipsoidal

1991 *Mathematics Subject Classification*. Primary 65D32, 33C50; Secondary 78M16, 65Y20.

Research supported in part by NSF grant SI2-SSI: 1450339 and DOE Contract DE-AC02-06CH11357.

coordinate system, definition of the harmonics, and define a problem in electrostatics which we will use as an illustration. In Section 3, we define tanh-sinh quadrature, and prove its optimality for calculation of the normalization constants. In Section 4, we detail our software implementation, and in Section 5 we demonstrate its effectiveness for some sample electrostatic problems.

2. BACKGROUND

This section provides the background necessary for our implementation of ellipsoidal harmonics, but further detail on ellipsoidal coordinates and harmonic solutions as they are used in this paper are available in [7] and [15]. Readers interested in further theory on ellipsoidal harmonics are encouraged to consult the book of Dassios [10] which provides a clear and comprehensive presentation.

2.1. Ellipsoidal Coordinates. The ellipsoidal coordinate system is a 3-dimensional generalization of the familiar 2-dimensional elliptic coordinate system. In these coordinates, the Laplacian is fully separable. Moreover, because ellipsoidal coordinates are defined with respect to a reference ellipsoid, it depends on the semi-axes a , b , and c for definition.

In an ellipsoidal system defined with respect to a reference ellipsoid with semi-axis lengths a , b , and c given by

$$(1) \quad \frac{x^2}{a^2} + \frac{y^2}{b^2} + \frac{z^2}{c^2} = 1,$$

an ellipsoidal point (λ, μ, ν) corresponding to Cartesian point (x, y, z) is given by the roots of

$$(2) \quad \frac{x^2}{s^2} + \frac{y^2}{s^2 - h^2} + \frac{z^2}{s^2 - k^2} = 1$$

where $h^2 = a^2 - b^2$ and $k^2 = a^2 - c^2$. The squares of the roots of Eq. (2) are contained in the intervals

$$(3) \quad \lambda^2 \in (k^2, \infty)$$

$$(4) \quad \mu^2 \in (h^2, k^2)$$

$$(5) \quad \nu^2 \in (0, h^2),$$

with the sign convention

$$(6) \quad \text{sgn}_\lambda = \text{sgn}_x \text{sgn}_y \text{sgn}_z$$

$$\text{sgn}_\mu = \text{sgn}_x \text{sgn}_y$$

$$\text{sgn}_\nu = \text{sgn}_x \text{sgn}_z.$$

Note that the inverse sign relation from ellipsoidal to Cartesian coordinates is given by swapping x for λ , y for μ , and z for ν in Eq. 6.

2.2. Ellipsoidal Harmonics. Analogous to spherical harmonics, interior ellipsoidal harmonics form a basis for square-integrable functions inside the reference ellipsoid. The Laplace equation is fully separable in ellipsoidal coordinates. If we assume a separable solution and plug that into the Laplacian, the one-dimensional functions in each variable satisfy Lamé's equation

$$(7) \quad (s^2 - h^2)(s^2 - k^2) \frac{d^2 E}{ds^2}(s) + s(2s^2 - h^2 - k^2) \frac{dE}{ds}(s) + (p - qs^2)E(s) = 0$$

where p and q are constants. Solutions to Lamé's equation fall into two classes: interior harmonics and exterior harmonics. These solutions are used to represent functions regular on the interior and exterior of the ellipsoid respectively. For a given order n , there are $2n+1$ interior harmonics each written as E_n^p for $p \in [0, 2n+1)$. These $2n+1$ solutions can be further divided into four sub-classes, K , L , M , and N to assist in calculation. For brevity, we will provide a brief overview of how solutions in class K are derived. Further details on the other classes are available in [7].

We assume that a given E_n^p in solution class K can be written in the form

$$(8) \quad E_n^p(s) = s^{n-2r} \sum_{j=0}^r b_j \left(1 - \frac{s^2}{h^2}\right)^j$$

where $r = \lfloor \frac{n}{2} \rfloor$. After plugging Eq. (8) into Eq. (7), further manipulation shows that the coefficients b_j are given as an eigenvector of a tridiagonal matrix, which depends on the solution class. Once these b_j coefficients have been determined, the harmonic E_n^p can be evaluated for different values of s using Eq. (8).

While the interior harmonics are unbounded as $\lambda \rightarrow \infty$, the exterior harmonics, F_n^p , are constructed such that $F_n^p(\lambda) \rightarrow 0$ as $\lambda \rightarrow \infty$. They are defined as

$$(9) \quad F_n^p(\lambda) = (2n+1)E_n^p(\lambda)I_n^p(\lambda)$$

where

$$(10) \quad I_n^p(\lambda) = \int_{\lambda}^{\infty} \frac{ds}{[E_n^p(s)]^2 \sqrt{s^2 - k^2} \sqrt{s^2 - h^2}}.$$

Notice that as $\lambda \rightarrow \infty$, $I_n^p \rightarrow 0$ faster than $E_n^p \rightarrow \infty$. Thus, F_n^p is guaranteed to decay towards 0 at infinity.

The normalization constants associated with ellipsoidal harmonics are defined by the surface integral

$$(11) \quad \gamma_n^p = \int \int_{\lambda=a} (E_n^p(\mu)E_n^p(\nu))^2 ds$$

which can be expressed in terms of μ and ν as

$$(12) \quad \int_0^h \int_h^k (E_n^p(\mu)E_n^p(\nu))^2 \frac{\mu^2 - \nu^2}{\sqrt{(\mu^2 - h^2)(k^2 - \mu^2)} \sqrt{(h^2 - \nu^2)(k^2 - \nu^2)}} d\mu d\nu$$

In order to compute this integral numerically, we use the following well-known decomposition into four one-dimensional integrals,

$$(13) \quad \gamma_n^p = 8(\mathcal{I}_1\mathcal{I}_2 - \mathcal{I}_3\mathcal{I}_4)$$

where

$$(14) \quad \begin{aligned} \mathcal{I}_1 &= \int_0^h \frac{(E_n^p(\nu))^2}{\sqrt{h^2 - \nu^2} \sqrt{k^2 - \nu^2}} d\nu & \mathcal{I}_2 &= \int_h^k \frac{\mu^2 (E_n^p(\mu))^2}{\sqrt{\mu^2 - h^2} \sqrt{k^2 - \mu^2}} d\mu \\ \mathcal{I}_3 &= \int_0^h \frac{\nu^2 (E_n^p(\nu))^2}{\sqrt{h^2 - \nu^2} \sqrt{k^2 - \nu^2}} d\nu & \mathcal{I}_4 &= \int_h^k \frac{(E_n^p(\mu))^2}{\sqrt{\mu^2 - h^2} \sqrt{k^2 - \mu^2}} d\mu \end{aligned}$$

We will directly compute these one-dimensional integrals using tanh-sinh quadrature.

2.3. Ellipsoidal Mixed Dielectric Model. In order to test the accuracy and efficiency of our method, we will use an ellipsoidal multipole expansion arising from the polarizable continuum model (PCM) of bioelectrostatics [5]. To allow for an explicit representation of the potential through an ellipsoidal harmonic expansion, we assume that the solvent is homogeneous, infinite, and isotropic, and also that the molecular cavity is ellipsoidal.

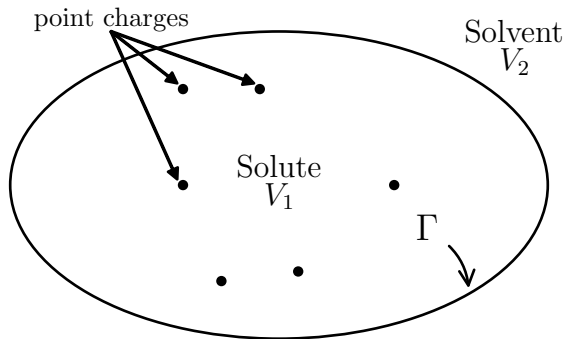


FIGURE 1. Mixed Dielectric Poisson Model

A diagram representing the model is shown in Fig. 1. The ellipsoidal boundary Γ separates solute cavity V_1 from the solvent region V_2 . The electric permittivities, ϵ_1 and ϵ_2 , are assumed to be constant inside and outside of the molecular cavity and thus discontinuous at boundary Γ . V_1 is also assumed to contain Q point charges each at position r_k with charge magnitude q_k for $k = 1, \dots, Q$.

Allowing Φ_1 and Φ_2 to represent the electric potentials in regions V_1 and V_2 respectively, we arrive at the following PDE:

$$(15) \quad \Delta\Phi_1(r) = \sum_{k=1}^Q q_k \delta(r - r_k)$$

$$(16) \quad \Delta\Phi_2(r) = 0$$

The boundary conditions relating Φ_1 and Φ_2 at Γ are the standard Maxwell boundary conditions: continuity of potential and electric displacement. For $r_s \in \Gamma$,

$$(17) \quad \Phi_1(r_s) = \Phi_2(r_s)$$

$$(18) \quad \epsilon_1 \frac{\partial \Phi_1}{\partial n}(r_s) = \epsilon_2 \frac{\partial \Phi_2}{\partial n}(r_s).$$

Finally, the electrostatic free energy due to solvation, $\Delta G_{\text{solv}}^{\text{el}}$ can be calculated directly from the interior solution for Φ_1 ,

$$(19) \quad \Delta G_{\text{solv}}^{\text{el}} = \frac{1}{2} \sum_{k=1}^Q q_k \Phi_1(r_k).$$

The physical interpretation of this model is that the solute charge distribution interacts with the dielectric medium by inducing an apparent surface charge with density $\sigma(r)$ on the boundary of the molecular cavity. Common PCM formulations obtain a solution for $\sigma(r)$ by discretizing over an equivalent boundary integral equation and solving the resulting

system numerically. The polarization field can then be calculated directly from $\sigma(r)$. The model above avoids direct discretization of $\sigma(r)$ by assuming an ellipsoidal cavity, so that the polarization field can be calculated using an expansion in ellipsoidal harmonics.

2.4. Ellipsoidal Multipole Solution. In order to derive an explicit multipole solution to our mixed-dielectric jump problem, we begin by assuming that the solution on the interior can be decomposed into a sum of the Coulomb potential plus the reaction potential due to the induced boundary charge distribution.

$$(20) \quad \Phi_1(r) = \psi^{\text{Coul}}(r) + \psi^{\text{reac}}(r)$$

We can use the well-known exterior expansion for the Green's function

$$(21) \quad \frac{1}{\|r - r'\|} = \sum_{n=0}^{\infty} \sum_{p=1}^{2n+1} \frac{4\pi}{2n+1} \frac{1}{\gamma_n^p} \mathbb{E}_n^p(r') \mathbb{F}_n^p(r)$$

which results in the following expansion for Coulomb potential valid for $\lambda \geq a$ (exterior and boundary points)

$$(22) \quad \psi^{\text{Coul}}(r) = \sum_{n=0}^{\infty} \sum_{p=1}^{2n+1} \frac{G_n^p}{\epsilon_1} \mathbb{F}_n^p(r)$$

where

$$(23) \quad G_n^p = \sum_{k=1}^Q q_k \frac{4\pi}{2n+1} \frac{1}{\gamma_n^p} \mathbb{E}_n^p(r_k).$$

If we then assume that ψ^{reac} and $\Phi_2(r)$ can be expanded in terms of interior and exterior harmonics

$$(24) \quad \psi^{\text{reac}}(r) = \sum_{n=0}^{\infty} \sum_{p=1}^{2n+1} B_n^p \mathbb{E}_n^p(r)$$

$$(25) \quad \Phi_2(r) = \sum_{n=0}^{\infty} \sum_{p=1}^{2n+1} C_n^p \mathbb{F}_n^p(r)$$

and then demand that $\Phi_1(r)$ and $\Phi_2(r)$ satisfy the boundary conditions in Eq. (17) and Eq. (18), and the Green's function expansion in Eq. (21) which is valid at the boundary, recognizing that the equation for each n is independent, we arrive at

$$(26) \quad B_n^p = \frac{\epsilon_1 - \epsilon_2}{\epsilon_1 \epsilon_2} \frac{F_n^p(a)}{E_n^p(a)} \left(1 - \frac{\epsilon_1}{\epsilon_2} \frac{\tilde{E}_n^p(a)}{\tilde{F}_n^p(a)} \right)^{-1} G_n^p$$

where

$$(27) \quad \tilde{E}_n^p(\lambda) = \frac{1}{E_n^p(\lambda)} \frac{\partial E_n^p(\lambda)}{\partial \lambda}$$

and \tilde{F}_n^p is defined analogously.

3. TANH-SINH QUADRATURE

Tanh-sinh quadrature is a numerical integration scheme for one-dimensional integrands on finite intervals and was specifically designed to handle endpoint singularities [20, 17]. Tanh-sinh works by first transforming an integrand on $(-1, 1)$ to $(-\infty, \infty)$ and then applying the uniform trapezoid rule to the resulting integrand. The change of variables for $t \in (-\infty, \infty)$, is given by

$$(28) \quad \psi(t) = \tanh\left(\frac{\pi}{2} \sinh t\right), \quad \psi'(t) = \frac{\frac{\pi}{2} \cosh t}{\cosh^2\left(\frac{\pi}{2} \sinh t\right)}.$$

Applying the truncated trapezoid rule with step size h then gives the formula for tanh-sinh:

$$(29) \quad \int_{-1}^1 f(x) dx \approx \sum_{k=-N}^N f(x_{kh}) w_{kh}$$

$$(30) \quad x_{kh} = \tanh\left(\frac{\pi}{2} \sinh kh\right), \quad w_{kh} = \frac{\frac{\pi}{2} h \cosh kh}{\cosh^2\left(\frac{\pi}{2} \sinh kh\right)}.$$

The efficiency of this formula is a result of two properties: the decay rate of the resulting integrand after transformation and the asymptotic optimality of the trapezoid rule for analytic integrals over \mathbb{R} . Due to the known optimality of the trapezoid formula for analytic integrals over the entire real line, the optimality of tanh-sinh and other similar quadratures depends on the efficiency of the change of variables. We begin by introducing a few function spaces commonly used in analysis of such quadratures.

3.1. Tanh-sinh Optimality. First we introduce \mathcal{D}_d to be a strip of finite width around the real axis in the complex plane defined by

$$(31) \quad \mathcal{D}_d = \{z \in \mathbb{C} \mid |\Im(z)| < d\}.$$

We have the following theorem credited to Tanaka et al. which provides a condition to tell whether an integrand under the tanh-sinh transformation falls into the function space characterized by Sugihara [19] in which tanh-sinh is optimal [21].

Theorem 1. *Assume that f is analytic in $\psi(\mathcal{D}_d)$ for some $d \in (0, \pi/2)$ and suppose there exists some $C_1 > 0$ and $\beta > 0$ such that $\forall z \in \psi(\mathcal{D}_d)$,*

$$(32) \quad |f(z)| \leq C_1 \left| (1 - z^2)^{\beta/2-1} \right|.$$

Then there exists some C independent from N such that

$$(33) \quad \left| \int_0^1 f(x) dx - h \sum_{k=-N}^N f(\psi(kh)) \psi'(kh) \right| \leq C \exp\left(-\frac{2\pi dN}{\log(8dN/\beta)}\right)$$

where

$$(34) \quad h = \frac{\log(8dN/\beta)}{N}$$

While it is relatively straightforward check whether many integrands are bounded by $|(1 - z^2)^{\beta/2-1}|$ on $(-1, 1)$, it is less straightforward to show this bound holds true on $\psi(\mathcal{D}_d)$ in Eq. (32). In Fig. 2, we show a contour plot of $\psi(\mathcal{D}_d)$ for $d = \pi/4$. In the following subsection, we prove that one of the normalization constant integrands lies in this space, before generalizing our proof in the next subsection.

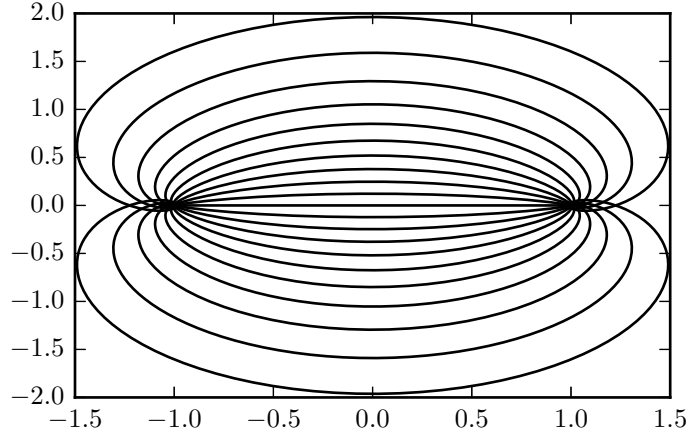


FIGURE 2. Contours of $\psi(\mathcal{D}_d)$. Each contour corresponds to a horizontal line in \mathcal{D}_d (imaginary part held constant).

3.2. The integral \mathcal{I}_1 . The intuition behind this proof is to show that the height d of the complex strip D_d can be chosen to be small enough such that all singularities outside the region of integration are excluded from the closure of $\psi(\mathcal{D}_d)$. This guarantees that the non-singular terms are continuous and thus bounded on $\psi(\mathcal{D}_d)$, giving us the necessary conditions for Theorem (1).

We start by looking at \mathcal{I}_1

$$(35) \quad \mathcal{I}_1 = \int_0^h \frac{(E_n^p(\nu))^2}{\sqrt{h^2 - \nu^2} \sqrt{k^2 - \nu^2}} d\nu$$

and transform this integral onto $(-1, 1)$ using the change of variables $z = \frac{2}{h}\nu - 1$ resulting in

$$(36) \quad \mathcal{I}_1 = \int_{-1}^1 \frac{E_n^p\left(\frac{h}{2}(z+1)\right)}{\sqrt{1 - \frac{(z+1)^2}{4}} \sqrt{k^2 - \frac{h^2(z+1)^2}{4}}} \frac{h}{2} dz.$$

The transformed integrand is continuous on \mathbb{C} with the exception of $z = 1$, $z = -3$, $z = \frac{2k}{h} - 1$, and $z = -\frac{2k}{h} - 1$. Thus, we want to choose d such that the latter three singularities are excluded from $\overline{\psi(\mathcal{D}_d)}$ so that the conditions for Theorem (1) are met.

Because ψ is Lipschitz for $d < \frac{\pi}{2}$, showing that the latter three singularities are excluded from $\overline{\psi(\mathcal{D}_d)}$ can be done by showing that the points in \mathbb{C} which map to singularities under ψ must be bounded away from the real axis, and thus can be excluded from \mathcal{D}_d . The following describes how this can be done by contradiction.

If we take ψ to be the tanh-sinh transformation and look at the set of points mapping to the latter three singularities,

$$(37) \quad S = \left\{ z \in \mathbb{C} \mid \psi(z) = -3 \text{ or } \psi(z) = \frac{2k}{h} - 1 \text{ or } \psi(z) = -\frac{2k}{h} - 1 \right\},$$

then we can show through contradiction that these must be bounded away from the real axis. Assuming for contradiction that they aren't bounded away from the real axis, there

exists a sequence of points $(x_j)_{j=1}^\infty$ where each $x_j \in S$ and $|x_j - \Re(x_j)| \rightarrow 0$ as $j \rightarrow \infty$. However, because ψ is Lipschitz, we know that $|\psi(x_j) - \psi(\Re(x_j))| \rightarrow 0$ as $j \rightarrow \infty$ as well. However, this is a contradiction because each $\psi(\Re(x_j)) \in (-1, 1)$ and $\psi(x_j)$ is a singular point of the integrand, implying that there is a sequence of singular points getting arbitrarily close to $(-1, 1)$ which is impossible with only three singular points. Therefore, if we choose $d = \inf(\Im(S))/2$, then $d > 0$ and by our choice of d , $\overline{\mathcal{D}_d} \cap S = \emptyset$.

Because $\overline{\mathcal{D}_d} \cap S = \emptyset$, the non-singular portion of our integrand contains no singularities and must be continuous on $\overline{\psi(\mathcal{D}_d)}$. Finally, because $\overline{\psi(\mathcal{D}_d)}$ is compact, this portion of our integrand is bounded by a constant resulting in the necessary conditions for Theorem (1).

Notice that this result doesn't rely on any specific properties of the non-singular portion of the integrand other than assuming it is analytic with a finite number of complex singularities. Thus, we can generalize this proof to functions of this type as is demonstrating in the following section.

3.3. General proof. For the following section,

$$(38) \quad \psi(z) = \tanh\left(\frac{\pi}{2} \sinh(z)\right)$$

Lemma 1. $\psi(z)$ is Lipschitz on \mathcal{D}_d whenever $d < \frac{\pi}{2}$

A proof of this algebraically is given in [21], but we provide a short proof based on Cauchy's derivative estimate. We present this proof because it only relies on the boundedness of ψ on \mathcal{D}_d and thus could easily be extended to other transformations.

Proof. First, we fix d arbitrarily such that $0 < d < \frac{\pi}{2}$. Then, given that ψ is bounded on \mathcal{D}_d for any $d < \frac{\pi}{2}$, there exists an M such that $|\psi(x)| \leq M$ on \mathcal{D}_d .

Cauchy's derivative estimate, a direct consequence of Cauchy's integral formula, states that if $|f(x)| \leq M$ on C , a circle of radius r centered at a , then

$$(39) \quad \left|f^{(n)}(a)\right| \leq \frac{n!M}{r^n}$$

Choosing an h such that $d < h < \frac{\pi}{2}$ and considering any $z \in \mathcal{D}_d$, we examine a circle C_z of radius $h - d$ centered at the point z . For any $y \in C_z$, we can apply the identity

$$(40) \quad \Im(y) = \Im(y - z) + \Im(z)$$

and because $|\Im(y - z)| \leq |y - z| \leq h - d$ and $z \in \mathcal{D}_d$, we have that

$$(41) \quad |\Im(y)| \leq |\Im(y - z)| + |\Im(z)|$$

$$(42) \quad |\Im(y)| < h$$

and therefore $C_z \subset \mathcal{D}_h$. By our original assumption we know that there exists some M_h such that $|\psi(x)| \leq M_h$ on \mathcal{D}_h . We have now shown that ψ satisfies the conditions for Cauchy's derivative estimate on the circle C_z for any $z \in \mathcal{D}_d$. Therefore, we have

$$(43) \quad |\psi'(z)| \leq \frac{M_h}{h - d}$$

in C_z . Furthermore, we observe that the right hand side of equation (43) is independent of z . This proves that ψ has bounded derivative on \mathcal{D}_d and as a consequence ψ is also Lipschitz on \mathcal{D}_d . \square

Lemma 2. $\psi(\mathcal{D}_d)$ is bounded.

Proof. Consider any point $z \in \psi(\mathcal{D}_d)$. By construction of this set, there exists some $x \in \mathcal{D}_d$ where $\psi(x) = z$. Furthermore, because ψ is Lipschitz, we have that $|\psi(x) - \psi(\Re(x))| = |z - \psi(\Re(x))| \leq L|x - \Re(x)| = L|\Im(x)| \leq Ld$. Thus,

$$(44) \quad |z - \psi(\Re(x))| \leq Ld$$

and $\psi(\Re(x)) \in (-1, 1)$, guaranteeing that any z arbitrarily chosen in $\psi(\mathcal{D}_d)$ is within a finite distance of $(-1, 1)$ independent of the choice of z . Therefore, $\psi(\mathcal{D}_d)$ is bounded. \square

The following theorem is our general result

Theorem 2. Consider $d \in (0, \frac{\pi}{2})$ and a function f of the form

$$(45) \quad f(x) = \frac{g(x)}{h(x)}$$

where f, g are analytic, the function h satisfies

$$(46) \quad |h(x)| \geq C_1 \left| \sqrt{1 - x^2} \right|$$

in $\psi(\mathcal{D}_d)$, and the function g is continuous on $[-1, 1]$ with a finite number of singularities in the complex plane.

Then f satisfies the conditions for Theorem (1).

Proof. We define S to be the points in \mathbb{C} which map to singularities of g under ψ i.e.,

$$(47) \quad S = \{z \in \mathbb{C} \mid g \text{ is singular at } \psi(z)\}.$$

We contend that the points in S are bounded away from the real axis. To show this, assume that they are not. Then, there exists a sequence of points $(z_k)_{k=1}^{\infty}$ where $z_k \in S$ and $|z_k - \Re(z_k)| \rightarrow 0$. Because ψ is Lipschitz, we have that $|\psi(z_k) - \psi(\Re(z_k))| \leq L|z_k - \Re(z_k)|$ for some constant L . From this inequality we can conclude that $|\psi(z_k) - \psi(\Re(z_k))| \rightarrow 0$ as well which is an infinite sequence of singular points of g getting arbitrarily close to points in the set $(0, 1)$. However, our original assumption that g is continuous on $[-1, 1]$ guarantees that $\psi(z_k)$ is not a limit point of $(-1, 1)$, allowing us to extract an infinite subsequence of unique points $(\psi(z_{n_k}))_{k=1}^{\infty}$ getting monotonically closer to the set $(-1, 1)$. The fact that this subsequence contains unique points contradicts our original assumption that g has finite singularities in the complex plane.

Therefore, the points in S are bounded away from the real axis i.e.,

$$(48) \quad \inf_{x \in S} |\Im(x)| > 0.$$

If we choose d to be $d := \frac{1}{2} \inf_{x \in S} |\Im(x)|$, then $\mathcal{D}_d \cap S = \emptyset$ and $\overline{\mathcal{D}_d} \cap S = \emptyset$. Furthermore, $\overline{\psi(\mathcal{D}_d)} \cap \psi(S) = \emptyset$ and due to Lemma (2), g must be bounded on the compact set $\overline{\psi(\mathcal{D}_d)}$ by some constant C_2 . This, combined with our original assumption in equation (46) that $h(x)$ is bounded below results in

$$(49) \quad |f(x)| = \frac{|g(x)|}{|h(x)|} \leq \frac{C_2}{C_1} \left| \frac{1}{\sqrt{1 - x^2}} \right|$$

as desired. \square

4. IMPLEMENTATION

Our ellipsoidal implementation follows [7] closely, but reimplements the functionality in C whereas the original used Python and MATLAB. In addition, we have used MPFR package [11] for arbitrary precision calculations. Our work has been integrated into the PETSc package [3, 4] from Argonne National Laboratory. The user can select either the fixed or arbitrary precision versions for a given integral. Dense linear algebra for the fixed precision version, such as the eigensolves used for harmonic initialization, were performed using LAPACK [1]. In the arbitrary precision version, linear algebra routines were implemented in MPFR and the eigenvalue problem was solved using a power iteration with reorthogonalization.

Coordinate transforms between the ellipsoidal and Cartesian systems were originally presented in [18] and further detailed in [7], which also presented a method for handling sign ambiguities (our Eq. (6)). We also follow [6] for the spherical harmonic implementation.

When initializing an ellipsoidal system and associated harmonics, abscissas (x_{kh}) and weights (w_{kh}) are precomputed for $k = -N, \dots, N$ where N is chosen so that $w_{Nh} \leq 10^{-2p}$ where p is the desired digits of precision, as recommended by Bailey [2]. The step size h used for initialization is $h_j = 2^{-j}$ where $j \in \mathbb{N}$ is provided by the user. Due to nested definition of tanh-sinh abscissas, this precomputation includes all abscissas computed with step size h_i for $0 \leq i < j$ up to the same 10^{-2p} tolerance for the weights.

The computational complexity associated with this initialization is $O(N)$ which contrasts Gaussian quadrature's $O(N^2)$ initialization cost using common approaches, although we do note the recent development of an $O(N)$ initialization scheme for Gaussian quadrature [12] albeit with larger constant. After initialization, the computational complexity associated with evaluating and accumulating N abscissa-weight pairs is $O(N)$ and the error decreases at a rate of $O\left(\exp(-c_1 \frac{N}{\log N})\right)$. After the abscissa/weight initialization, the inner trapezoid rule computation in tanh-sinh is implemented adaptively with the step size halved at each level. Convergence was assessed using the estimates provided by Bailey [2] which were uniformly close to the actual errors in tests.

5. RESULTS

5.1. Implementation Accuracy. In order to verify our computation of the normalization constants, we will compare to both explicit formulae (for degree up to two) and to a high precision MPFR implementation executed with approximately 1000-digit arithmetic. As implemented, normalization constants of an arbitrary order can be independently computed with accuracy only limited by the precision of interior harmonic evaluation. As demonstrated in Fig. 3, the double precision calculation is accurate for low-order harmonics, but the accuracy degrades for high-order harmonics.

In order to examine the efficiency of the tanh-sinh transformation, we compare it to two popular transformations: error function and tanh. Because quadrature nodes and weights can be precomputed for many applications, we choose to compare accuracy against the number of function evaluations. In Fig. 4, we see that tanh-sinh is not only more efficient, but has a higher rate of convergence.

5.2. Ellipsoidal Potential Problems. The so-called Born ion, a single charge at the center of a dielectric sphere, provides a verification of our overall energy calculation. We construct a nearly spherical cavity and look at the limit as its becomes a sphere. In Fig. 5, we consider a single unit point charge at the origin and cavity semi-axes of lengths $a = 1 + \Delta$,

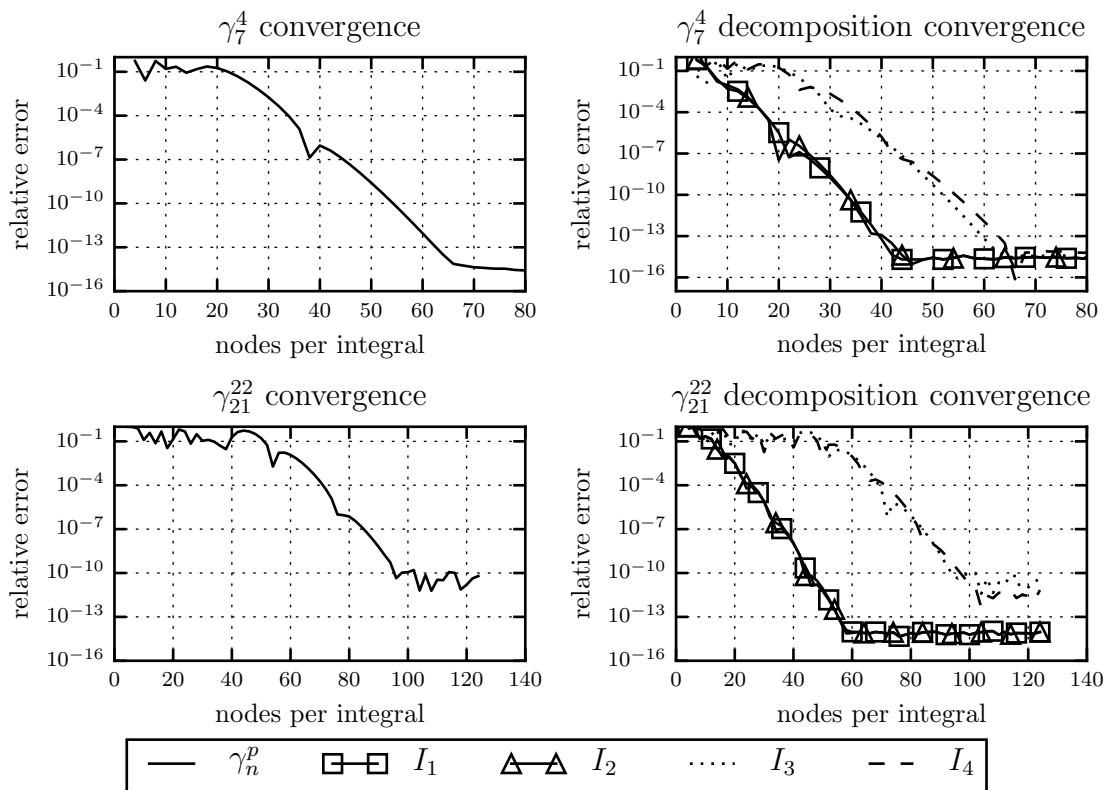


FIGURE 3. Convergence of normalization constants for ellipsoid with $a=3$, $b=2$, $c=1$.

$b = 1 + \Delta/5$, $c = 1 + \Delta/10$ as $\Delta \rightarrow 0$. We see that the free energy converges linearly to that of the Born ion.

We would also like to examine the convergence of our expansion for the simple problem of an ellipsoidal cavity with semi-axis lengths $a = 3$, $b = 2$, $c = 1$ and five randomly placed interior charges. As shown in Fig. 6, the solvation free energy, $(\Delta G_{\text{solv}}^{\text{el}})$, converges exponentially with respect to the maximum order of expansion, as expected. In the work-precision diagram, we see that convergence is sublinear with respect to flops due to the nonlinear relationship between work required and order of expansion. However, it is worth mentioning that most calculations performed to generate this solution can be trivially parallelized.

For approximately ellipsoidal charge distributions, the ellipsoidal expansion can have a substantially larger region of convergence. For the same ellipse and charge configuration as above, we show the convergence of spherical and ellipsoidal expansions in Fig. 7. In order to compare solutions, we only examine the Coulomb portion of each potential. In the left figure, we see that the ellipsoidal expansion convergences for points outside the containing ellipse, but inside the Brillouin Sphere, which is the smallest sphere containing the charges.

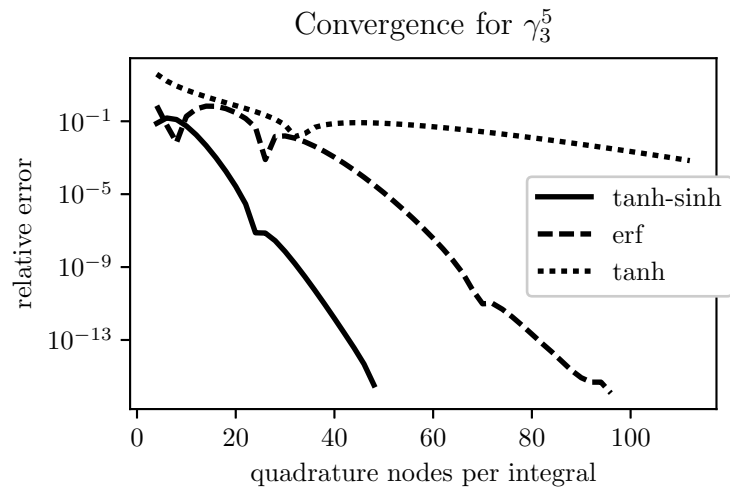


FIGURE 4. Comparison of three integral transforms for the computation of a fifth order normalization constant.

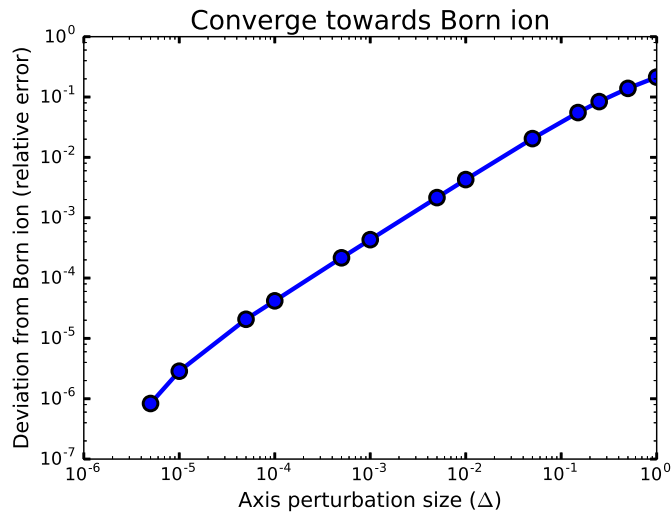


FIGURE 5. Error in free energy against the Born ion as cavity becomes spherical.

6. DISCUSSION

We have provided simple implementation capable of accurately calculating ellipsoidal harmonic expansions at least to order 50. We make use of tanh-sinh quadrature, taking advantage of adaptivity in the algorithm, which may be easily coded by the user, but we also make available a free C implementation in the PETSc source [4, 3]. We have demonstrated a superior convergence rate from ellipsoidal harmonics, and more robust convergence when

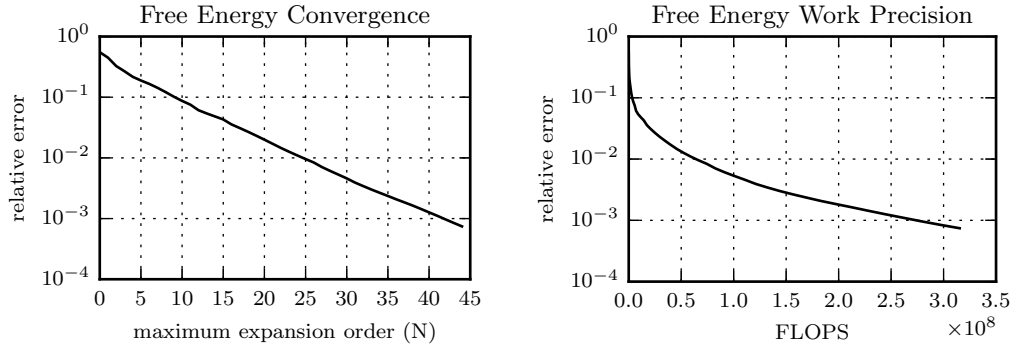


FIGURE 6. Convergence and work-precision diagrams for the free energy of an ellipsoidal cavity with 5 randomly placed charges.

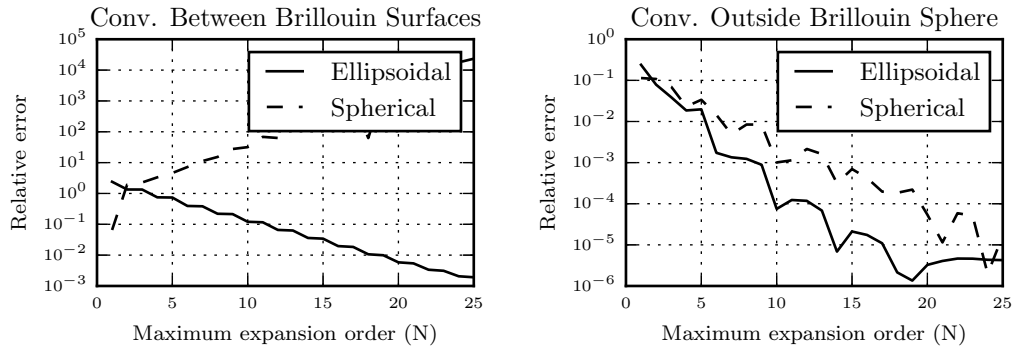


FIGURE 7. Convergence of the Coulomb potential for spherical and ellipsoidal expansions for the potential due to an ellipsoidal distribution of charge, at a point inside the sphere containing the charge but outside the ellipsoid (left) and a point outside both the sphere and ellipsoid (right).

sources are better enclosed by an ellipsoid. We hope this enables spectral methods based on ellipsoidal harmonics as a viable alternative to the more common spherical harmonic expansion.

More broadly, it seems that our approach to optimality of the quadrature can be applied to other classes of singular integrals, for examples those that make up the Galerkin boundary element method. Currently, analytic integrals or quadratures specialized to the kernel or geometry are often used, but this seems to provide an automatable method for attacking the problem, which might be complementary to the QBX approach [14]. We also believe that the spectral method for the PCM using ellipsoidal harmonics could be used as a valuable supplement to operator approximation methods for the solvation problem [8, 6].

REFERENCES

- [1] E. ANDERSON, Z. BAI, C. BISCHOF, L. S. BLACKFORD, J. DEMMEL, J. J. DONGARRA, J. DU CROZ, S. HAMMARLING, A. GREENBAUM, A. MCKENNEY, AND D. SORESENSEN, *LAPACK Users' Guide (Third Ed.)*, Society for Industrial and Applied Mathematics, Philadelphia, PA, USA, 1999.
- [2] D. H. BAILEY, K. JEYABALAN, AND X. S. LI, *A comparison of three high-precision quadrature schemes*, *Experimental Mathematics*, 14 (2005), pp. 317–329.
- [3] S. BALAY, S. ABHYANKAR, M. F. ADAMS, J. BROWN, P. BRUNE, K. BUSCHELMAN, L. DALCIN, V. EIJKHOUT, W. D. GROPP, D. KAUSHIK, M. G. KNEPLEY, L. C. MCINNES, T. MUNSON, K. RUPP, B. F. SMITH, S. ZAMPINI, H. ZHANG, AND H. ZHANG, *PETSc users manual*, Tech. Rep. ANL-95/11 - Revision 3.7, Argonne National Laboratory, 2016.
- [4] ———, *PETSc Web page*. <http://www.mcs.anl.gov/petsc>, 2017.
- [5] J. P. BARDHAN, *Biomolecular electrostatics—I want your solvation (model)*, *Computational Science & Discovery*, 5 (2012), p. 013001.
- [6] J. P. BARDHAN AND M. G. KNEPLEY, *Mathematical analysis of the BIBEE approximation for molecular solvation: Exact results for spherical inclusions*, *Journal of Chemical Physics*, 135 (2011), pp. 124107–124117. <http://arxiv.org/abs/1109.0651>.
- [7] ———, *Computational science and re-discovery: open-source implementations of ellipsoidal harmonics for problems in potential theory*, *Computational Science & Discovery*, 5 (2012), p. 014006. <http://arxiv.org/abs/1204.0267>.
- [8] J. P. BARDHAN, M. G. KNEPLEY, AND M. ANITESCU, *Bounding the electrostatic free energies associated with linear continuum models of molecular solvation*, *Journal of Chemical Physics*, 130 (2008), p. 104108. Selected for the March 15, 2009 issue of *Virtual Journal of Biological Physics Research*, <http://dx.doi.org/10.1063/1.3081148>.
- [9] W. E. BYERLY, *An elementary treatise on Fourier's series: and spherical, cylindrical, and ellipsoidal harmonics, with applications to problems in mathematical physics*, Dover, 1893.
- [10] G. DASSIOS, *Ellipsoidal harmonics: theory and applications*, vol. 146, Cambridge University Press, 2012.
- [11] L. FOUSSE, G. HANROT, V. LEFÈVRE, P. PÉLISSIER, AND P. ZIMMERMANN, *MPFR: A multiple-precision binary floating-point library with correct rounding*, *ACM Transactions on Mathematical Software (TOMS)*, 33 (2007), p. 13.
- [12] A. GLASER, X. LIU, AND V. ROKHLIN, *A fast algorithm for the calculation of the roots of special functions*, *SIAM Journal on Scientific Computing*, 29 (2007), pp. 1420–1438.
- [13] E. W. HOBSON, *The theory of spherical and ellipsoidal harmonics*, CUP Archive, 1931.
- [14] A. KLÖCKNER, A. BARNETT, L. GREENGARD, AND M. ONEIL, *Quadrature by expansion: A new method for the evaluation of layer potentials*, *Journal of Computational Physics*, 252 (2013), pp. 332–349.
- [15] T. KLOTZ, *Accurate evaluation of ellipsoidal harmonics using tanh-sinh quadrature*, Master's thesis, Computational and Applied Mathematics, Rice University, Houston, TX, 2017.
- [16] W. MILLER, JR, *Symmetry and separation of variables*, Addison-Wesley Publishing Co., Inc., Reading, MA, 1977.
- [17] M. MORI, *Discovery of the double exponential transformation and its developments*, *Publications of the Research Institute for Mathematical Sciences*, 41 (2005), pp. 897–935.
- [18] G. ROMAIN AND B. JEAN-PIERRE, *Celestial Mechanics and Dynamical Astronomy*, 79 (2001), pp. 235–275.
- [19] M. SUGIHARA, *Optimality of the double exponential formula - functional analysis approach -*, *Numerische Mathematik*, 75 (1997), pp. 379–395.
- [20] H. TAKAHASI AND M. MORI, *Double exponential formulas for numerical integration*, *Publications of the Research Institute for Mathematical Sciences*, 9 (1974), pp. 721–741.
- [21] K. TANAKA, M. SUGIHARA, K. MUROTA, AND M. MORI, *Function classes for double exponential integration formulas*, *Numerische Mathematik*, 111 (2008), pp. 631–655.

(Matthew Knepley) DEPARTMENT OF COMPUTATIONAL AND APPLIED MATHEMATICS, RICE UNIVERSITY,
HOUSTON, TX 77005
E-mail address: knepley@rice.edu

(Thomas Klotz) DEPARTMENT OF COMPUTATIONAL AND APPLIED MATHEMATICS, RICE UNIVERSITY, HOUSTON,
TX 77005
E-mail address: tsk1@rice.edu

(Jaydeep Bardhan) DEPARTMENT OF MECHANICAL ENGINEERING, NORTHEASTERN UNIVERSITY, BOSTON,
MA 02115

E-mail address: jbardhan@neu.edu